Author response to the review of Young et al. “Rapid and accurate polarimetric radar measurements of ice crystal fabric orientation at the Western Antarctic Ice Sheet (WAIS) Divide deep ice core site” [Manuscript # tc-2020-264]

We would like to thank the two reviewers, Martin Rongen and Reinhard Drews, for their thorough, thoughtful and constructive reviews. Please find below the two reviewers’ comments (RC) in **bold**, each followed by the authors’ response (AC). Line, figure, and page numbers mentioned by the reviewers (within RC) refer to the original manuscript. The proposed changes to a future version of the manuscript are underlined. We note that we have not yet implemented these proposed changes and therefore the actual implementation of these Author Comments may vary somewhat from what is stated below.

Review by Martin Rongen (30 October 2020)

General comments

RC1.1. The authors present a quad-polarimetric radar measurement at WAIS Divide. The dataset is interesting in its innovative nature as well as in the quality of the derived results. The method follows in direct succession to earlier works developed by Shuji Fujita and Tom Jordan among others. While previous measurements required a manual rotation of the antenna system in small steps in order to measure the azimuthal variation associated with the birefringence signature, the quad-polarimetric measurement allows for signal at arbitrary azimuths to be deduced from just four antenna orientations. The results are validated by comparison to ice core data.

The overall presentation is detailed and rigorous. Some improvements may be made by giving a clearer structure to the results and discussion sections (see later specific comments). As a non-expert on glaciological radar measurements, the theory and methods section was challenging but the provided references proofed to be very helpful. For the paper to stand on its own some more context/details may be added (see specific comments). Some more discussion may also be added to section 5.3 (Methods comparisons and limitations). It currently gives a fair comparison between radar and ice core / sonic measurements but is short on the specific limitations and assumptions involved in generating data for arbitrary azimuth angles using the quad-polarimetric data.

AC1.1. Thank you for your detailed review, and you as well as Reinhard Drews have correctly identified that we need to further discuss some method comparisons and limitations. We hope that we’ve addressed your concerns in the specific comments section below.

Specific comments

RC1.2. The readability of the results section would be greatly improved by structuring it in sub-sections, as is also done for the other sections. A possible structure could be:

- **– 4.1 Experimental results from WAIS (up to line 224)**
- **– 4.2 Modelling the observed data (lines 224-255)**
- **– 4.3 Fabric asymmetry estimation (lines 255 ff)**

AC1.2. Thank you for these suggestions. We will implement them in the revised manuscript.

RC1.3. The meaning of the pad factor mentioned in line 193 is unclear.

AC1.3. The pad factor refers to the amount of zero-padding applied to the time-domain signal. We apply zero-padding to our data with a pad factor of 2, as recommended by Brennan et al. (2014). While zero-padding is a common application in signal processing, we will make it explicit that the pad factor refers to the amount of zero padding equivalent to the total length of the signal.

RC1.4. The details and reliability of the firn correction as introduced in line 198 are unclear. It is mentioned that this correction amplifies the estimated $E_2 - E_1$ values in the shallow ice and surprisingly large fabric asymmetries are then measured in that depth range. Thus the firn correction merits more attention (and maybe test without the correction) during the discussion (line 265 and 305) may be warranted.

AC1.4. We implement firn correction as suggested in the Appendix of Jordan et al. (2020a). Because the equation that drives this correction was derived from founding ice-penetrating radar principles (e.g. the ice-air volume fractions in the mixing relations of Looyenga 1965), we believe these corrections to be physically representative of firn anisotropy. Notwithstanding, we agree with your belief that the fabric asymmetries in firn are surprisingly large. Therefore, we will: (i) make a new figure (tentatively Figure 5) that shows near-surface $E_2 - E_1$ with and without firn correction; (ii) clarify why we apply firn correction in our revised manuscript (i.e. the reasoning given above); and (iii) attempt to address the physical origins and implications of high anisotropy in snow and firn, in particular, considering the effects of firn densification on crystal rotation (e.g. Burr et al. 2017) which, though the end member is a vertical pole, would therefore induce azimuthal anisotropy when considering the non-limiting case.

RC1.5. In line 196 it may be worth mentioning that the Jordan et al. (2019) prescription to evaluate $d\varphi_{hhvv}/dz$ is not actually based on the phase plot itself but on the real and imaginary components of the coherence as given in equation 7b.

AC1.5. We will implement this suggestion and clarify our methods in the revised manuscript.

RC1.6. The reasons for and consequences of switching from an FIR filter to the method described in l.197ff remain unclear.

AC1.6. We had used our method (a 2-D median filter + 2-D peak convolution) in a previous paper that processes 2-dimensional (x-z and y-z) imagery from a multistatic pRES array (Young et al. 2018). The reason for using this then was to remove high-frequency noise and

speckle. We have also visually checked the filtered image to ensure that there are no remaining “rapid phase excursions due to a modulo 2π artefact” (Dall 2010). Therefore, we are confident that the goals of our method are comparable to those of Jordan et al. (2019). We are happy to apply the FIR filter in the revised manuscript if you still believe it to be necessary to do so.

RC1.7. The anisotropy parameter β seems to be missing a unit (dB?) in the caption of Figure 3.

AC1.7. You are correct. We will correct this omission in the revised manuscript.

RC1.8. For depth greater than 1200 m (and to a lesser extent around 600 m) the derived $E_2 - E_1$ values become rather unstable. While this is commented on and partially reflected in larger error bars, a population of outliers with small fabric asymmetries as well as small error bars is a bit worrying. It may be beneficial to show a plot of the coherence magnitude. Given vanishing magnitudes, the phase becomes unconstrained leading to erratic $d\varphi_{hhvv}/dz$ values. In the deepest region the phase in Figure 2.e is more unstable as a function of depth than expected from the model calculation.

AC1.8. We agree with your suggestion to include $|c_{hhvv}|$. At the same time, because the antenna polarisation plane is aligned with the ice optic axis along all sites (see AC2.3 for the location of all ApRES measurement sites). Your hypothesis that the outliers in Figure 4 correspond to small $|c_{hhvv}|$ is correct: beyond 1300 m, values of $|c_{hhvv}|$ are generally <0.4. We propose to add a plot of $|c_{hhvv}|$ in either Figure 2 or Figure 4 to constrain the validity of these outliers (the exact form to be determined upon resubmission). We will set an appropriate $|c_{hhvv}|$ bound to use to filter outliers, which will change the visualisation of Fig. 2e and 4 somewhat.

RC1.9. The sentence "The birefringence of an individual crystal and its COF are related to the bulk ..." in line 97 reads a bit odd as a COF only applies to an ensemble of crystals. Maybe change to something like "the birefringence of individual crystals and their COF".

AC1.9. Your suggestion is good, and we will implement this in the revised manuscript.

RC1.10. The term "depth step" in line 124 is a bit technical. Something like "depth where a reflection occurs" would be clearer to the reader.

AC1.10. We will replace “... for each depth step and azimuthal orientation” with “... at each discrete scattering layer and azimuthal orientation”, which is in line with the terminology used by Fujita et al. (2006) in their Section 2.2.

RC1.11. The meaning and relevance of the rotation matrix *R* as introduced in line 133 is unclear. To my understanding, it represents the rotation of the COF principle axis *of each traversed ice layer* with respect to a reference system defined by the antennas.

AC1.11. You are correct: the rotation matrix R is used in Equation (1) to reconstruct the theoretical signal components for each azimuthal shift θ, for which the component in question is either T (transmission between the antennas and the scattering layer) or Γ (reflection at the scattering layer). The use of R in essence replicates an azimuthal-rotational experiment (acquisitions made at each rotational increment of the antenna acquisition plane). Your suggestion to clarify the use of R is valid, and we will summarise the above explanation and add this as a statement at the end of the paragraph in question.

RC1.12. It is mentioned that s_{hv} and s_{vh} should be identical given an ideal measurement. Has the difference between these two orientations been studied and the potential impact quantified?

AC1.12. In theory, $s_{hv} = s_{vh}$ which is well known according to the Lorentz reciprocity theorem. In practice, there will be small differences including (but not limited to): (i) differences in the beam pattern between the transmitting and receiving aerials, (ii) random clutter within the transmitted media; and (iii) human error in antenna positioning. This topic is well studied (e.g. there is a 100+ page book (Stumpf 2017) purely dedicated to antenna signal reciprocity!) but in general, the main differences between s_{hv} and s_{vh} are due to human error during data collection. In general, our data has minimal difference between s_{hv} and s_{vh}, although there is some additional variability seen at the near surface (Figure AC1). This discrepancy may account for the mismatch between measured (Figure 2b,c,d) and modelled co-polarised results (Figure 3a,b,c) in the top ~200 m. We will modify Figure 2a (which already includes s_{vv} and s_{vh} incorrectly labelled as e_{vv}, e_{vh}, which we will correct in our revised manuscript) to also include s_{hv} and s_{vv} to show how the Lorentz Reciprocity Theorem works in practice. We will also state this discrepancy in the results and mention our hypothesis in the discussion.

Additionally, sometimes $s_{hv} = -s_{vh}$ due to the 180° ambiguity in antenna position. This is true in our case, and we explain why and the ramifications to the output polarisation plots (specifically Figure 2b and 2c) in AC2.3).

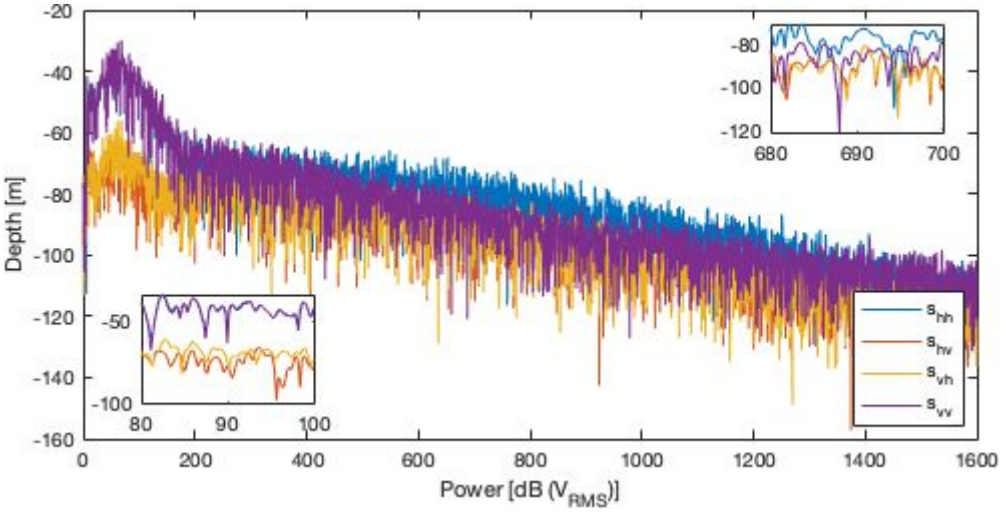

Figure AC1. Mean (polarisation-averaged) power return for each antenna orientation. Insets show magnification of power returns.

RC1.13. The COF orientation of each depth layer is resolved "by tracing the azimuthal minima in the cross-polarized power anomaly". While this may be a good approximation for this measurement, I wonder if this technique is generally applicable in the presence of strongly varying COF orientations. Assuming, for example, a constant angle of 20° in the top 500 m and a constant angle of 60° below, my understanding is that the minimum in the cross-polarized power anomaly would only slowly migrate towards 60° below 500 m as the bulk propagation is initially still dominated by the conditions above. One essentially measures the average COF orientation up to the scattering depth. But there may be a misunderstanding on my part here. A comment would be appreciated.

AC1.13. In general, this method (as well as other published methods so far, e.g. Brisbourne et al. 2019, Jordan et al. 2020a) is accurate if the COF orientation is depth invariant. If the orientation undergoes an abrupt switch, such as the example that you propose above and below 500 m, the minima in power anomaly would similarly undergo an abrupt switch (e.g. at ~215 m in Figure 4 of Brisbourne et al. 2019). If this happens, the 90° ambiguity in the cross-polarised power anomaly plot would need to be resolved by either the co-polarised power anomaly or the co-polarised phase difference plots (see AC2.19). If the orientation undergoes a slow rotation, the identified ice optic axis from the cross-polarised minima method is lagged from the true fabric orientation (e.g. Column 3, Figure 4c of Jordan et al. 2020c). The inaccuracy in identification of the ice optic axis will then result in corresponding over- or under-estimation of fabric asymmetry (e.g. Column 4, Figure 4c of Jordan et al. 2020c).

We will summarise the above paragraph in the Discussion (see AC2.2 of how exactly we will incorporate this within suggestions to include other relevant limitations).

RC1.14. As noted in the general comments section 5.3 would benefit from a discussion of the specific limitations and assumptions involved in generating data for arbitrary azimuth angles using the quad-polarimetric data.

AC1.14. See AC2.4 for a discussion on the comparisons between quad-polarimetric and azimuthal rotational experiments.

RC1.15. Section 5.1 paragraph 2 (lines 281-288) seems better suited in section 4.1 (results, modeling), here a Figure similar to Figure 5 in the Fujita 2006 paper may also be illustrative, showing that birefringence results in nodes in the power anomalies while anisotropic scattering results in a band structure, the spacing of which is a function of the scattering strength.

AC1.15. While a figure similar to Figure 5 of Fujita et al. (2006) may be useful, this specific figure has already been reproduced multiple times in subsequent papers (e.g. Figure 7 of Matsuoka et al. 2012, Figure 2 of Brisbourne et al. 2019) and we feel like there is already enough literature that describes the depth and azimuthal variability of the co-polarised nodes. Furthermore, we believe that Figure 3 already serves the same purpose, in particular, a comparison between Figure 3b and 3d which shows the controls of anisotropic scattering (β) and birefringence ($\varepsilon(z)$, through E_2-E_1). We will however add a sentence at L246 that

explicitly states that the azimuthal fabric asymmetry (as a representation of birefringence) is proportional to the depth-periodicity of co-polarised nodes. We will also move Section 5.1 Paragraph 2 (L281-288) to Section 4.1 which we agree is a good suggestion.

Technical comments

RC1.16. The link for the Mott, H. (2006) reference appears to be dead.

AC1.16. Thank you for pointing this out. We will fix the link.

RC1.17. In line 156, spectra so should be plural as are the amplitudes.

AC1.17. We will implement this correction in the revised manuscript.

RC1.18. In the title of subsection 5.1 it would be more consistent to refer to "anisotropic scattering" instead of the more ambiguous "anisotropy"

AC1.18. We agree with this suggestion and will implement this in the revised manuscript.

Review by Reinhard Drews (19 November 2020)

Summary

RC2.1. In their paper ”Rapid and accurate polarimetric radar measurements of ice crystal fabric orientation at the Western Antarctic Ice Sheet (WAIS) Divide deep ice core site”, Young and co-authors present an ApRES radar dataset, which they use to infer the ice-fabric characteristics continuously to a depth of 1500 m. Main results include quantification of the horizontal ice anisotropy with a depth invariant ice-fabric orientation that is aligned with the directions of the principal strain rates. The inferences are validated with data from the WAIS ice core, and some conclusions are drawn about the ice-divide stability throughout the Holocene.

Overall, this paper is nicely written and the authors do a commendable job in guiding the reader through the methods and results. However, in places I find the paper unnecessarily superficial and I don't see novel aspects clearly. I also suspect (but I am not certain) that parts of the azimuthal reconstruction may be erroneous leading to wrong inferences in terms of the ice-fabric orientation. Below, I mention a number of major comments/questions how this can be improved. Applications of radar polarimetry are still rare, and I hope that the points raised below will help to improve the next version of this paper.

AC2.1. Thank you for your detailed review, and we appreciate your honesty in that you have disclosed your potential conflict of interest. We believe your review is unbiased and correctly identifies several areas will need to be addressed, specifically the three major comments (RC2.2 - 2.4). We have attempted to alleviate your concerns in our responses below. Ultimately, we hope that our paper can contribute to the radar polarimetry literature and

RC2.2. Clarify methodological advance

It is stated that this study "..extends previous qualitative analyses [...] to obtain quantitative measurements.." (l. 285). Can you highlight more clearly what those extensions were compared to previous studies? From what I can see so far, this study nicely applies previous developments to a single new site, but I struggle to see the extensions. The link between the polarimetric phase gradient and ice- fabric parameters is based on the cited papers Fujita et al., 2006 and Jordan et al., 2019. Arguably matching the angular distance of co-polarization nodes with a 2D optimisation is new (l.233), but at least the dependency of this distance as a function of anisotropic scattering is already approximated in Fujita 2006. Also advantages or pitfalls (e.g., in terms of uniqueness and uncertainties involved) of this approach are not discussed.

I suppose that this paper is the first to explicitly focus on synthesising quad-polarimetric measurements for ApRES, although the related methodology is known from radar polarimetry textbooks (e.g., the cited Mott, 2006). The inferences drawn from this method about the ”high angular” resolution are not credible as currently presented (see comment below). Also the lack of rotational dataset at this

site makes it hard to discuss advantages/disadvantages of both approaches. I suggest a dedicated section were improvements and distinct differences compared to previous studies are highlighted more explicitly.

AC2.2. In our opinion, this manuscript extends the literature (this being radar polarimetry for glaciological applications) through: (i) validation of co-polarised power anomaly and phase difference plots; (ii) publication of the quad-polarimetric reconstruction method; and (iii) direct validation of radar-derived measurements of ice fabric to that of ice cores at high depth resolution. We are fortunate that our results are simple to comprehend, and we believe that this, combined with the straightforward layout of the quad-polarimetric reconstruction method will help those who wish to apply radar polarimetric methods to glaciology. Due to the growing interest in radar polarimetry applications within the glaciological community as of late, we believe that our manuscript is not only valuable, but also timely for the above three reasons. In detail:

> (i) is shown through the direct comparison between measured (Figure 2) and modelled (Figure 3) results, where the birefringence in the latter was induced using fabric eigenvalues from thin-section analysis of ice cores. (The anisotropic reflection ratio is instead estimated through matching the locations of the co-polarised nodes and the four-quadrant patterns with the measured results.) While we concede that the theory behind this comparison has previously been quantified in Fujita et al. (2006), they stop short of presenting modelled results complementary to their observations (in their case, fabric data from the Mizuho and Dome Fuji ice cores). Similarly, while fabric measurements from polarimetric radar measurements have been verified to ice core data by Jordan et al. (2019), they implement only the polarimetric coherence method (i.e. analysis of s_{hhvv}) and do not present any co- or cross-polarised datasets. On the other hand, Brisbourne et al. (2019) present co-polarised power anomaly and phase difference plots of radar measurements conducted at Korff Ice Rise but focus on the relative orientation of the antenna polarisation plane relative to the ice optic axis, and present only qualitative observations in terms of fabric strength. Our manuscript not only directly compares measured results to modelled plots, but also quantifies azimuthal fabric strength through the polarimetric coherence method and verifies results directly with ice core data. Therefore, our manuscript reconciles the methods of the above three studies.
>
> Regarding (ii), we felt a need to include the complete equations that show how the received signal (both power in Equation 4 and phase in Equation 5) can be reconstructed from quad-polarimetric measurements. You are correct in that these methods are established, and we do not attempt to take credit for them. However, these methods are often presented within dense literature specifically directed towards radar engineering applications and may be daunting for the majority of glaciologists (myself included!). Rather, we attempt to introduce them to the glaciological literature in an approachable format so that they are easily accessible for researchers wishing to conduct quad-polarimetric experiments.
>
> Regarding (iii), our results show that choosing a nominal depth-averaging window of 15 m (which is our nominal bulk-depth resolution) when applying the polarimetric coherence method (Equation 6) produces estimates of azimuthal fabric asymmetry

that closely match corresponding results from ice-core thin section data at similar resolutions (See AC2.7 regarding the specific use of the word 'resolution'). While Jordan et al. (2019) also use the polarimetric coherence method to match fabric asymmetry estimates between radar and ice core measurements, also showing comparative results, they had chosen to use a conservative nominal depth resolution of 100 m. Our study shows that this nominal depth resolution can be reduced down to levels at or exceeding that of the vertical spacing of ice core thin sections, while still producing comparable results.

As you may already know, there are multiple pitfalls in using the polarimetric coherence method, which are detailed in Jordan et al. (2019) and (2020a). We do not wish to regurgitate what has already been said, but we acknowledge that we have provided little caveats, which makes it seem like we are "overselling" our results. Therefore, we will separate Section 5.3 (Method comparisons and limitations) into two sections: (i) Method comparisons; and (ii) Advantages and limitations of the polarimetric coherence method. In the latter, we will summarise the pitfalls mentioned in Jordan et al. (2019) and (2020a), as well as other observations in our dataset, for example, the issue of symmetry at 90° if the wrong signs are used (see RC and AC2.3). We will also summarise the three advantages listed in the previous three paragraphs in this section.

RC2.3. Coincidental symmetry at θ = 90°?

In Figs. 2b-e one principal axis of the ice-fabric appears at the local azimuthal angle θ = 90° (i.e., all panels have a reflectional or rotational symmetry around the θ = 90° axis). This means that during measurements antennas were coincidentally placed parallel (*hh*) and perpendicular (*vv*) to the (at the time) unknown ice-fabric orientation. It is possible that the operators in the field made a conscious decision here because θ = 90° aligns with the strain rate (not the ice-flow) direction. However, given uncertainties involved in determining the direction of maximum strain rate and the antenna orientation, the θ = 90° symmetry almost seems too much of a coincidence. Based on our own experience with analysing quad-polarimetric data, we suggest that the authors double-check that indeed $s_{hv} = s_{vh}$. We found occasionally that $s_{hv} = -s_{vh}$ without satisfying explanation as to why this can be the case (e.g., inconsistencies in labelling and naming of antenna orientations in the field?). However, if it is the case, then reconstruction of the ApRES signal using eq. (4) forces a symmetry axis at θ = 90° exemplified below for the s_{hh} component:

$$S_{11} = s_{hh}(\theta) = \underbrace{\underbrace{s_{hh}\cos^2\theta + s_{vv}\sin^2\theta}_{\text{symmetric at } \theta=90^\circ} + \underbrace{(s_{vh}+s_{hv})\sin\theta\cos\theta}_{\text{anti-symmetric at } \theta=90^\circ}}_{\text{in general no symmetry axis at } \theta=90^\circ \text{ unless } s_{hv}=-s_{vh}}$$

The graphic below illustrates how this would be reflected in a full azimuthal reconstruction where the principal axis around θ = 35, 125° in the top plot are erroneously mapped to θ = 90, 180°. Without a co-polarized, rotational dataset this will occur unnoticed.

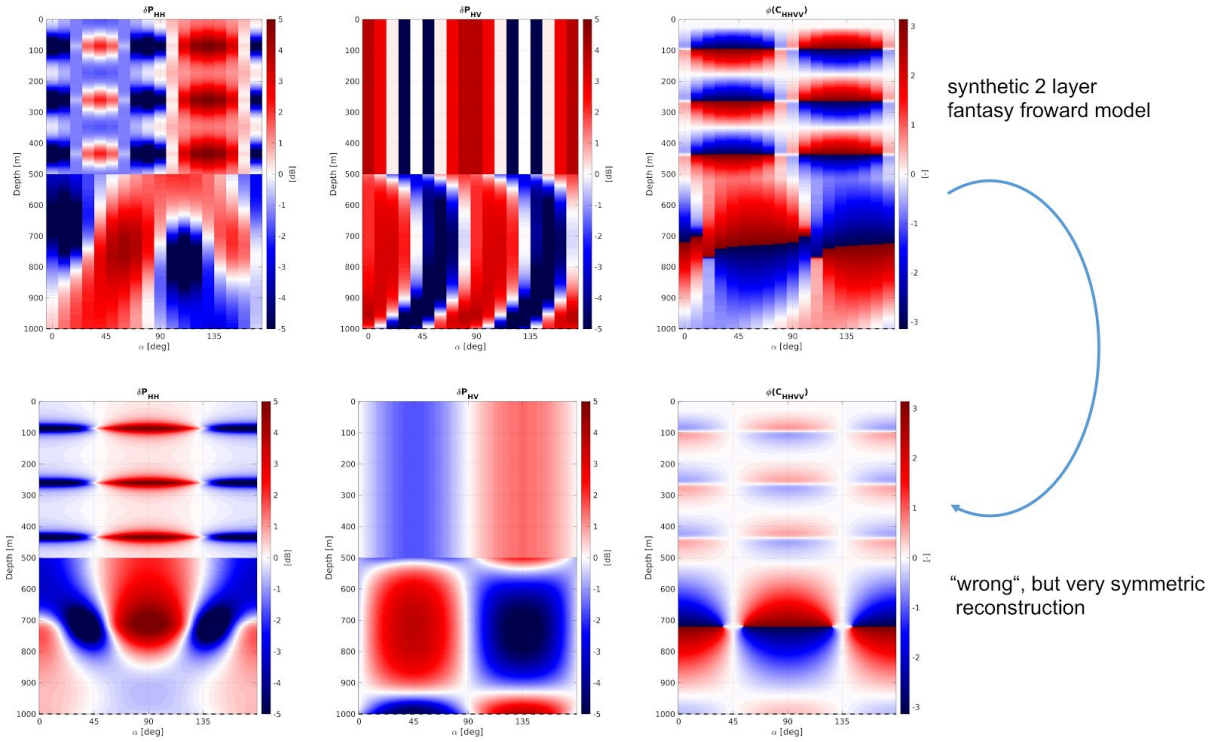

Maybe it will be helpful to investigate this further. Alternatively, state explicitly how the *hh* and *vv* directions were defined in the field, and why it makes sense that those axis align almost perfectly with the principal directions of the ice-fabric.

AC2.3. Your suspicions in the exact alignment of the antenna polarimetry plane in Fig. 2 with the strain axes is warranted. In our initial manuscript submission, we show the results from one ApRES site, but we did not mention in our manuscript that we had also obtained ApRES measurements from nine other sites along a ~6 km-long transect. The results displayed in Fig. 2 represents Site I, and is one of 10 total sites in terms of their relative position along the transect. The antenna axis (i.e. the plane that runs between the transmitting and receiving antenna) is orthogonal to the transect line, which is shown in Figure (AC2a).

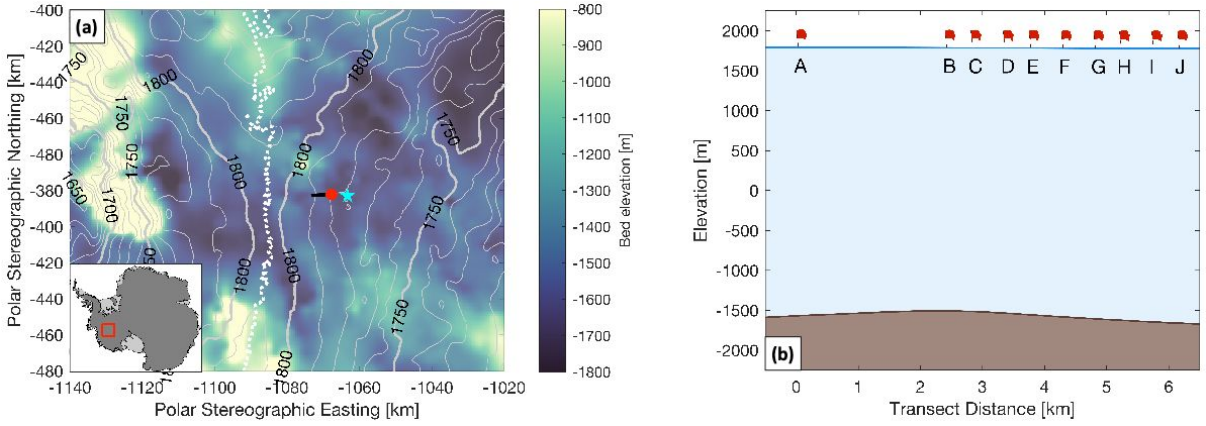

Figure AC2. (a) Map of local surface (grey contours) and basal topography (background colour) in the WAIS Divide area. Map is equivalent to Figure 1 with the addition of the ApRES transect. The red dot shows Site I where the data that produced Figure 2 was collected. (b) Surface and bed topography along the ApRES transect showing the relative locations of the 10 ApRES measurement sites.

Surface topography was obtained from REMA (Howat et al. 2019) and bed topography from BedMachine Antarctica v1 (Morlighem et al. 2020).

Upon re-inspection of our code, we have noticed a rounding error when importing the Northing and Easting coordinates that resulted in the antenna polarisation plane to be aligned exactly with the direction of maximum compression. In reality, the antenna polarisation plane is actually +7° (where positive numbers represent counterclockwise directions) from the strain compressive axis (rounded to the nearest degree).

Using data collected at Site I (the data used to produce Figure 2 in the initial TCD manuscript), we present in Figure (AC3) 2 sets of plots of co- and cross-polarised power anomaly and phase difference. Set 1 (panels a) assumes that $s_{hv} = s_{vh}$, and set 2 (panels b) assumes $s_{hv} = -s_{vh}$. In these figures, the mean and standard error of the principal axis for panels (a) were calculated to be 89.7° ± 0.05°, and for panels (b), 90.3° ± 0.09°, using the same methods described in the TCD manuscript. Figure (AC3) shows that the principal axis is indeed oriented at 90° (given appropriate rounding of significant figures).

However, because the two results give approximately the same results, we are not able to determine whether or not panels (a) or (b) shows the correct polarimetric patterns from Figure (AC3) alone. We then run the same investigation on the other 9 sites and show the output plots from one of these sites (Site C) in Figure (AC4). We regard the results shown in Figure (AC4) to have higher variability between results produced using each of the two assumptions in turn, but overall representative of all sites. We note three differences in Figure (AC4) that are not immediately obvious in Figure (AC3). First: for all sites, the first assumption that $s_{hv} = s_{vh}$ will always produce a symmetric co-polarised power anomaly and phase difference plot about $\theta = 90°$. Second: we note that the principal axis inferred solely from the co-polarised plots using this first assumption is misaligned with the principal axis as determined from the cross-polarised power anomaly. Third: the principal axes in all plots produced under the second assumption that $s_{hv} = -s_{vh}$ are all consistent with each other. For the example site (Site C) shown in Figure (AC4), the plots produce a principal axis oriented at 81.1° ± 0.07° under the first assumption ($s_{hv} = s_{vh}$, Figure AC4a) and 101.8° ± 0.09° under the second assumption ($s_{hv} = -s_{vh}$, Figure AC4b). We assume that the deviation of the principal axis from exactly 90° in both assumptions is the result of human errors in antenna positioning. The reflectional symmetry in the orientation of the principal axis (i.e. ~ -10° from 90° with the first assumption and ~ +10° from 90° with the second assumption at Site C) is seen at all sites, which reflects the importance of knowing whether an increase in azimuth in the polarimetry plots corresponds to a clockwise or anticlockwise rotation in antenna orientation.

Assuming that the four orthogonal combinations of antenna orientations were conducted in the same way for all 10 sites (which, to the best of our knowledge, is true), the results from Figure (AC3) and Figure (AC4) show that (i) the positions of [h | v] and [v | h] that we used in the field (Figure 1a) correspond to the second assumption that $s_{hv} = -s_{vh}$; (ii) the use of the cross-polarised power anomaly in determining the principal axis is valid regardless of whether the first or second assumption is used; and (iii) the principal axis for Site I at 90° and aligned exactly with the strain axes is valid as well as being fortuitous. At the same time, you will notice that Figure (AC3a1-3) are the mirror images to Figure (2b-d) in the TCD

manuscript. This is because we had implemented the first assumption ($s_{hv} = s_{vh}$) upon submitting to TCD, where positive differences between the ice optic axis and the antenna polarisation plane results in clockwise rotation. This error was initially not obvious because of the apparent symmetry of the *hh* and *hv* plots about 90°. After discussion with co-authors, we modified the code so that positive differences now reflect counterclockwise rotation, which is in line with the convention used for polar coordinates. We apologise for the confusion caused.

Therefore, given the new knowledge gleaned from this investigation, we will implement the following in our revised manuscript draft: (a) update our estimate of relative orientation of the ice optic axis from 0 to +2° (and a statement that we have rounded to the nearest degree); (b) re-process our datasets using the assumption that $s_{hv} = -s_{vh}$; (c) provide equivalent plots of Figure 2 for the other 9 sites in Supporting Information to show consistency across the entire transect; (d) provide an explanation in Section 3.3 as to why the principal axis is aligned almost exactly with the strain compression axis; and (e) provide a statement in Section 3.4 that details the importance of checking whether $s_{hv} = s_{vh}$ or $s_{hv} = -s_{vh}$. We very much thank you for pointing out to check the assumptions of symmetric reciprocity; otherwise, we would have published erroneous results!

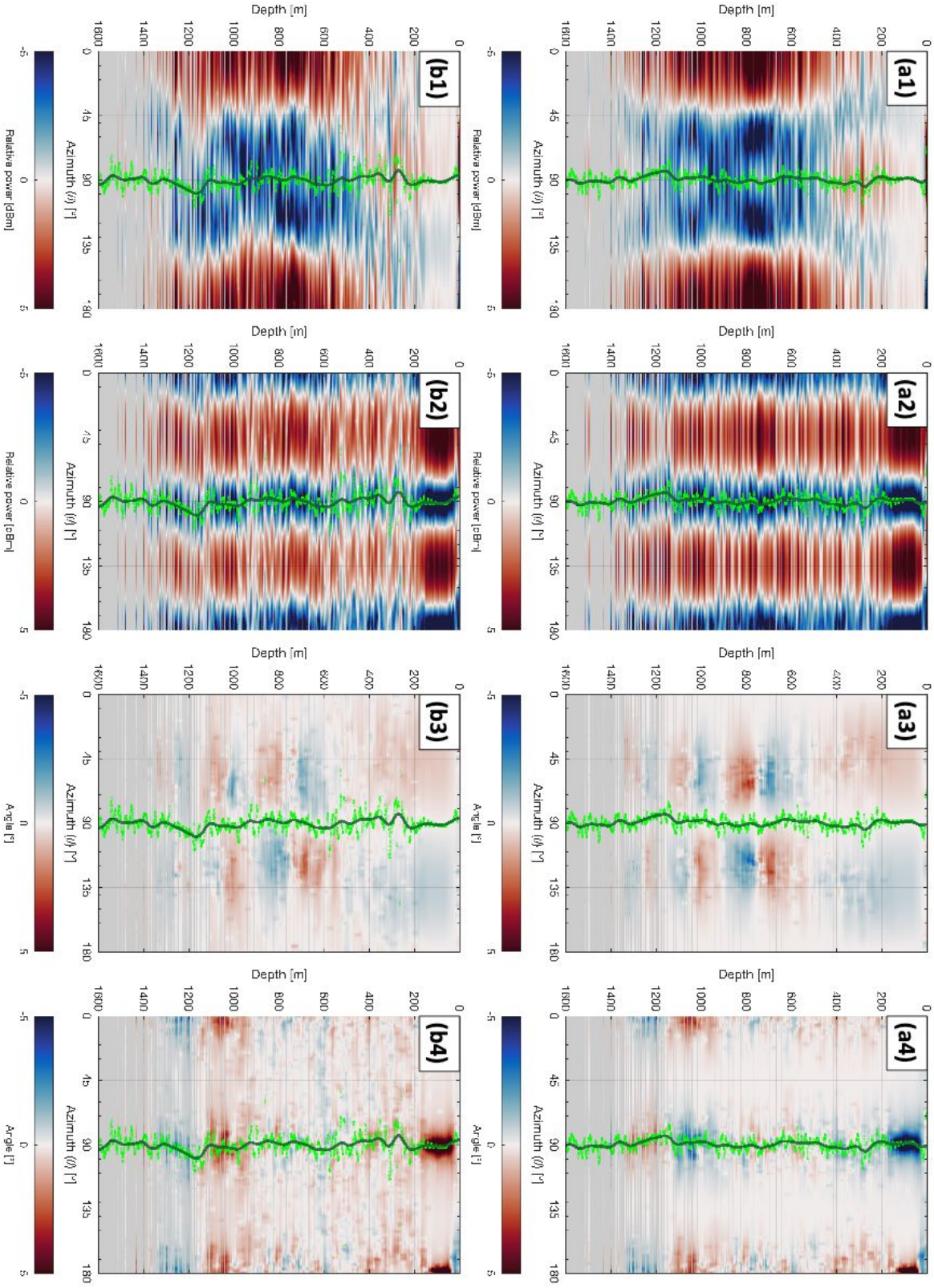

Figure AC3. ApRES polarimetric power anomaly and phase difference measured at Site I, WAIS Divide (Figure AC2). The top row of panels (a) were produced assuming $s_{hv} = s_{vh}$, and the bottom row of panels (b) assume $s_{hv} = -s_{vh}$. Columns (1) show co-polarised power anomaly, columns (2) cross-polarised power anomaly, columns (3) co-polarised phase difference, and columns (4) cross-polarised phase difference. Bright green dots represent azimuthal minima at each range bin, and the dark green line is the best estimate of the symmetry axis calculated using a

Gaussian-weighted moving average of the azimuthal minima. Depths with insufficient SNR are greyed out.

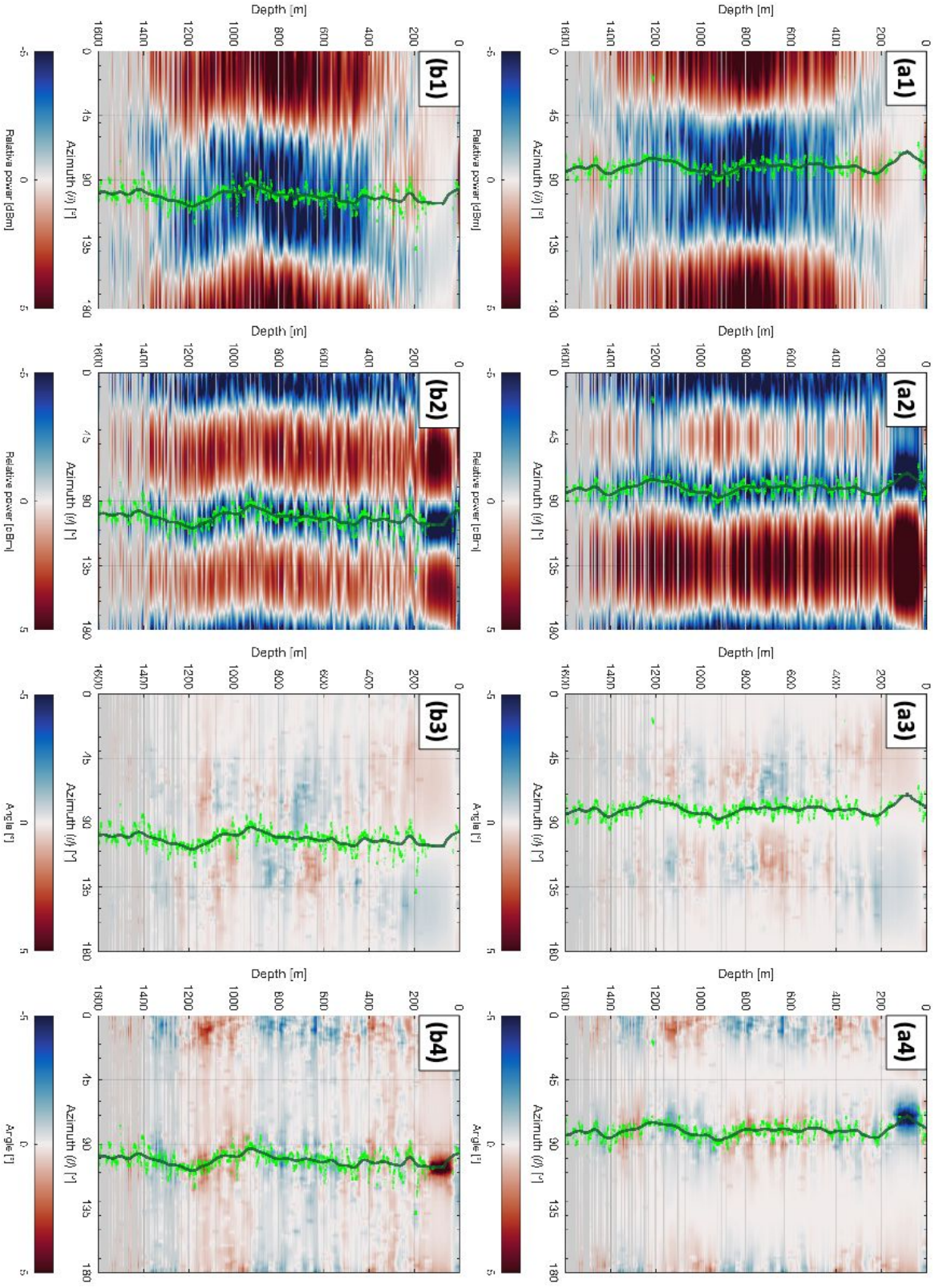

Figure AC4. ApRES polarimetric power anomaly and phase difference measured at Site C, WAIS Divide. Legends are identical with those for Figure AC3.

RC2.4. Terminology linked to azimuthal resolution

In numerous instances (e.g., l.7, l39, l49..) the authors advertise that synthesizing the azimuthal response from quad-polarimetric data (eq. 4) results in improved angular resolution compared to rotational setups. I disagree with that. The chosen azimuthal spacing of 1° (l. 397) is completely arbitrary and any value works with eq. 4. I agree that advantages and disadvantages of quad- polarimetric vs. rotational measurements should be discussed, but choosing an arbitrary gridding for θ is not enough in this regard. Also, no rotational dataset is presented so that the claims about the superiority of quad-polarimetric measurements are not rigorously substantiated (apart from the obvious fact that they are much quicker to obtain).

AC2.4. Unfortunately we did not conduct azimuthal rotational measurements at WAIS Divide and so we are unable to make a full and direct comparison between quad-polarimetric and rotational measurements specifically with regards to our own datasets at WAIS Divide. However, comparisons between the two field methods were made when analysing ApRES data from Brisbourne et al. (2019) of which we found minimal difference in the results generated from the two methods.

That being said, Matsuoka et al. (2012) conducted an azimuthal rotational survey close to (~5 km from) our study site of which the results are shown in their Figure 3, Panel SW-24. Although they had used radar systems with different frequencies from ours (60 and 179 MHz as opposed to 300 MHz for ApRES), we can see that, at least to 1400 m, our estimate of the fabric orientation matches their results.

We acknowledge that we cannot fully claim the superiority one measurement method over the other without conducting both at the same study site, and so we will mention the caveat in that, because we did not conduct azimuthal rotational measurements, we are unable to make a full and direct comparison between the two methods. Because of this caveat, we will drop the claims of azimuthal resolution superiority from using quad-pol measurements. We will then qualitatively compare our results to that of Matsuoka et al. (2012) to show that, visually, the results are similar. We will also mention that from analysis of experiments conducted at Korff Ice Rise, we observe that the produced results are qualitatively similar (C. Martin, unpublished data).

Minor remarks

RC2.5. Abstract should state limitation that the methodology only works if one of the c-axis is pointing upwards.

AC2.5. That is a fair point and we will make this limitation explicit in the abstract.

RC2.6. l 57: Eq. 4 reconstructs the azimuthal response, but this is something different than resolving it. See comments above.

AC2.6. See AC2.4.

RC2.7. l 63: Specify what resolution you refer to. ApRES surely has lower potential for vertical resolution than ice-core data.

AC2.7. ApRES certainly has lower resolution potential than ice-core data and we apologise for not being specific. The issue with defining the vertical resolution of ice cores is due to allocation of core sections to different scientific goals (at least, to the best of my knowledge), so while the depth resolution of ice cores in terms of fabric eigenvalue estimates can potentially be down to the centimeter scale, in practice the thin sections used to estimate eigenvalues are taken at larger intervals (~50-100m for the WAIS Divide ice core). The depth resolution of ApRES refers to the bulk-averaged fabric of the local depth window (15 m in our case). We propose to distinguish the two by using the term “bulk-averaged depth resolution” for the vertical resolution of ApRES measurements of ice fabric, and “depth separation” for the corresponding measurements of ice-core thin sections. Following the terminology of Jordan et al. (2019), we will modify this sentence to state: “... at a nominal bulk-averaged depth resolution of 15 m. We show that, using this setup and method, our estimates of fabric asymmetry are comparable to that from ice cores taken at similar depth intervals. From our results, we determine…”.

RC2.8. l 65: Specify what the angular resolution is. It cannot be the 1° . I would also prefer more modest wording for ”unambiguously”. Defining the direction of the ApRES antennas alone is already error-inflicted and there is no rigorous statement in this paper on how this was done.

AC2.8. We will replace “unambiguously identify” with “explicitly determine”. Because there is ambiguity in the attribution of angular resolution to either the model azimuthal bin size (1°) or the accuracy of orienting the antennas, we choose to instead remove “...to high angular resolution” from this sentence.

RC2.9. Overall nice structure of the introduction. This works for me.

AC2.9. Thanks for the compliment!

RC2.10. Fig. 1a include orientation of the E-field vector. Statement that antennas are oriented parallel to the divide is conflicting with inference that principal axis is at θ = 90° (which is parallel to flow, which is oblique to the divide according to Fig 1b). See major comment 2.

AC2.10. We will include the orientation of the E-field vector in Figure 1 in the revised manuscript. The angle stated here (250°) is actually the orientation of the velocity vectors and should instead state 268°. We will correct this in the future manuscript, and calculate uncertainties for this angle from human error (see RC2.18 for how we will calculate this).

RC2.11. l 114 not only ice-dynamics but also ice properties induced through climate variations imprint on the ice-fabric evolution. I am not sure the principal ice-fabric axis always line up with today’s strain rate regime as suggested here.

AC2.11. We acknowledge the effect of climate variations on climate history, however, although we have some idea of how climate can perturb the magnitude of fabric from Kennedy et al. (2013), its influence in influencing its orientation remains unclear (to the best of my knowledge). Therefore, we respectfully choose to not take your suggestion on including the role of climate perturbation in this statement. We will however reduce the certainty of this sentence, which will now read: "The direction of the greatest horizontal c-axis concentration in general reflects the orientation of horizontal strain extension and corresponds with E_2 in our notation.

RC2.12. l 127 the terminology "anisotropy" for β has confused me. You also need "anisotropy" for birefringence. Why not call it the "anisotropic reflection ratio" or something like that? "boundary reflection" is more appropriate than "boundary scattering" (the latter suggests some diffuse scattering which is not accounted for in this context. However, this may be a matter of taste.)

AC2.12. We will take your suggestion and rename β as the "anisotropic reflection ratio".

RC2.13. l 137 remove abbreviation SISO. It is not used later on.

AC2.13. We will remove abbreviation "SISO" in the revised manuscript.

RC2.14. l 150 include uncertainties for this angle here and elsewhere.

AC2.14. See AC2.10.

RC2.15. l 169 double-check that $s_{vh} = s_{hv}$ (see comment above).

AC2.15. We address this comment in AC2.3.

RC2.16. I understand how this azimuthal phase difference is calculated, but I don't understand what the additional value is. What inferences are drawn from the co-polarised phase difference that cannot be drawn from the hhvv phase angle?

AC2.16. The four-quadrant patterns in the co-polarised (*hh*) phase difference plots are coincident with the location of the nodes in the co-polarised power anomaly plots (Brisbourne et al. 2019). The location of these nodes and four-quadrant patterns then constrains the 90° ambiguity in the cross-polarised (*hv*) power anomaly (See AC2.19). We find it to be more clear to locate the nodes and check the fabric orientation using a combination of investigating the co-polarised nodes and four-quadrant patterns (as in Brisbourne et al. 2019) than in the *hhvv* phase angle plot. Having the co-polarised power anomaly and phase difference plot may be useful in case of an abrupt shift in fabric orientation (again, as evidenced in Brisbourne et al. 2019).

We acknowledge that we may not have made our above method clear in the manuscript. We will summarise the above explanation when describing our method of identifying and resolving the fabric orientation at the end of Section 3.4.

RC2.17. l 193 This first paragraph is more methods to me than results.

AC2.17. We will move the sentences “A pad factor of 2… with the same moving matrix dimensions.” to Section 3.3.

RC2.18. As stated above the 90° are suspicious. Also, what are the ±7° based on? I would think that errors in antenna positioning are larger.

AC2.18. In AC2.3, we state that the 90° is accurate. The ±7° is the 95% confidence interval (mistakenly attributed as standard error in the manuscript, which we will correct). The confidence interval was calculated from the ensemble of estimates of axis orientation at each depth bin (azimuthal minima, bright green dots in Figure 2). These errors are unrelated to antenna positioning. To address your concern, in the future revised manuscript, we will incorporate errors in antenna positioning by calculating the deviation of the symmetry axis from 90° for all 10 measurement sites (under assumption that (i) the flow regime and the resulting fabric at all sites are similar and therefore oriented in the same direction; and (ii) antennas were oriented in the same direction at each site, which we state in AC2.3, with deviations resulting from human error in antenna positioning).

RC2.19. l 213 Typo? This ambiguity cannot be resolved in the *hh* power anomaly shown in Fig 2b. You need to use the polarity of the phase gradient.

AC2.19. On the contrary: if anisotropic scattering is present in the imaged ice, the 90° ambiguity in the cross-polarised (*hv*) power anomaly can be resolved by determining either (i) the azimuthal minima of the co-polarised (*hh*) power anomaly plot, or (ii) the azimuth of the centre of the four-quadrant patterns in the co-polarised phase difference plots, as stated in Section 5.1 of Brisbourne et al. (2019). If co-polarised nodes are weak due to strong anisotropic scattering, the sign reversals in the four-quadrant patterns remain diagnostic.

On the other hand, if there is no anisotropic scattering present, then both the co-polarised power anomaly and phase difference plots will present 90° ambiguity as shown in Figure 2a of Brisbourne et al. (2019).

Because we observe at least moderate levels of anisotropic scattering in our observations (i.e. $1 \leq \beta \leq 5$ in Figure 3), we stand by our belief that the use of the *hh* power anomaly and phase difference plots to resolve the 90° ambiguity in the *hv* power anomaly is a valid technique.

RC2.20. l 221 at least estimate these “human” errors

AC2.20. See AC2.18 for how we will estimate and incorporate human errors in antenna positioning.

RC2.21. why is the “anisotropy” an integer value?

AC2.21. Apologies. β (the anisotropic scattering parameter in the manuscript, now termed the anisotropic reflection ratio) should have units of dB. Because anisotropic scattering is poorly constrained, we restricted our model fitting to only using integer values and interpolated through depth between points to avoid overfitting the data.

RC2.22. l 237 I think I missed something here: Aren't those node pairs simply depths where the phase shift between ordinary and extraordinary wave is odd integer multiple of π ? Clearly they will have a correspondence in the azimuthal phase difference (which is directly related to the phase angle). I don't understand the deeper physical implication of this 'four quadrant pattern yet.

AC2.22. See AC2.16 for further discussion on the relevance of the co-polarised phase difference.

RC2.23. Fig. 4 I appreciate the error bars on the ApRES derived $E_2 - E_1$. Please state more clearly how those were derived.

AC2.23. We state our error calculation in L187 (using the Cramer-Rao bound to obtain the associated phase error of $d\phi_{hhvv}/dz$, and following the ensemble method of Jordan et al. 2019). E_2 - E_1 is obtained directly through $d\phi_{hhvv}/dz$, and the error is then transferred accordingly. We will modify L187 to explicitly state that we calculate the phase error of $d\phi_{hhvv}/dz$, which then transfers accordingly to uncertainties for each E_2 - E_1 depth bin.

RC2.24. l 289 This is not the "best model" that matches observed results. It is a model that explains some of the features in the observations

AC2.24. We will implement this correction in the revised manuscript.

RC2.25. l 330 How fast does the ice-fabric structure adapt to a new strain regime? I think some sort of statement in this regard is required to better justify statements of ice-divide stability.

AC2.25. Brisbourne et al. (2019) states that, although the time taken to overprint a preexisting fabric is dependent on temperature, strain rate, and stress regime, it is poorly constrained excluding those from laboratory results. Recent results by Lilien et al. (in review) suggest that it takes tens of thousands of years to overprint fabric (assuming that lattice rotation dominates the fabric evolution, as most evidence indicates). Therefore, we can implement the same reasoning as that of Brisbourne et al. (2019) and state that the measured COF distribution aligned with the observed surface strain orientation through depth reflects the current ice flow regime, assuming that the vertical assumption (i.e. E_2 - E_1) holds through the range of measured depths. We will add these above statements to the revised version of our manuscript.

References

Brennan, P. V., Nicholls, K. W., Lok, L. B., and Corr, H. F. J.: Phase-sensitive FMCW radar system for high-precision Antarctic ice shelf profile monitoring, IET Radar, Sonar & Navigation, 8, 776–786, https://doi.org/10.1049/iet-rsn.2013.0053, 2014.

Brisbourne, A. M., Martín, C., Smith, A. M., Baird, A. F., Kendall, J. M., and Kingslake, J.: Constraining Recent Ice Flow History at Korff Ice Rise, West Antarctica, Using Radar and Seismic Measurements of Ice Fabric, Journal of Geophysical Research: Earth Surface, 124, 175–194, https://doi.org/10.1029/2018JF004776, 2019.

Burr, A., Noël, W., Trecourt, P., Bourcier, M., Gillet-Chaulet, F., Philip, A., and Martin, C. L.: The anisotropic contact response of viscoplastic monocrystalline ice particles, Acta Materialia, 132, 576–585, https://doi.org/10.1016/j.actamat.2017.04.069, 2017.

Dall, J.: Ice sheet anisotropy measured with polarimetric ice sounding radar, in: 30th International Geoscience and Remote Sensing Sympo- sium (IGARSS 2010), pp. 2507–2510, Honolulu, HI, https://doi.org/10.1109/IGARSS.2010.5653528, 2010.

Fujita, S., Maeno, H., and Matsuoka, K.: Radio-wave depolarization and scattering within ice sheets: A matrix-based model to link radar and ice-core measurements and its application, Journal of Glaciology, 52, 407–424, https://doi.org/10.3189/172756506781828548, 2006.

Horgan, H. J., Anandakrishnan, S., Alley, R. B., Burkett, P. G., and Peters, L. E.: Englacial seismic reflectivity: Imaging crystal-orientation fabric in West Antarctica, Journal of Glaciology, 57, 639–650, https://doi.org/10.3189/002214311797409686, 2011.

Howat, I. M., Porter, C., Smith, B. E., Noh, M.-J., and Morin, P.: The Reference Elevation Model of Antarctica, The Cryosphere, 13, 665–674, https://doi.org/10.5194/tc-2018-240, 2019.

Jordan, T. M., Schroeder, D. M., Castelletti, D., Li, J., and Dall, J.: A Polarimetric Coherence Method to Determine Ice Crystal Orientation Fabric From Radar Sounding: Application to the NEEM Ice Core Region, IEEE Transactions on Geoscience and Remote Sensing, pp. 1–17, https://doi.org/10.1109/tgrs.2019.2921980, 2019.

Jordan, T. M., Schroeder, D. M., Elsworth, C.W., and Siegfried, M. R.: Estimation of ice fabric within Whillans Ice Stream using polarimetric phase-sensitive radar sounding, Annals of Glaciology, 61, 74–83, https://doi.org/10.1017/aog.2020.6, 2020a.

Jordan, T. M., Martin, C., Brisbourne, A. C., Schroeder, D. M., and Smith, A. M.: Radar characterization of ice crystal orientation fabric and anisotropic rheology within an Antarctic ice stream, Earth and Space Science Open Archive ESSOAr, pp.1-48, https://doi.org/10.1002/essoar.10504765.1, 2020c.

Kennedy, J. H., Pettit, E. C., and Di Prinzio, C. L.: The evolution of crystal fabric in ice sheets and its link to climate history, Journal of Glaciology, 59, 357–373, https://doi.org/10.3189/2013JoG12J159, 2013.

Looyenga, H.: Dielectric constants of heterogeneous mixtures. Physica, 31, 401–406, https://doi.org/10.1016/0031-8914(65)90045-5, 1965.

Lilien, D. A., Rathmann, N. M., Hvidberg, C. S., and Dahl-Jensen, D.: Modeling ice-crystal fabric as a proxy for ice-stream stability, Journal of Glaciology, pp. 1-37, in review.

Matsuoka, K., Power, D., Fujita, S., and Raymond, C. F.: Rapid development of anisotropic ice-crystal-alignment fabrics in- ferred from englacial radar polarimetry, central West Antarctica, Journal of Geophysical Research: Earth Surface, 117, 1–16, https://doi.org/10.1029/2012JF002440, 2012.

Morlighem, M., Rignot, E., Binder, T., Blankenship, D., Drews, R., Eagles, G., Eisen, O., Ferraccioli, F., Forsberg, R., Fretwell, P., Goel, V., Greenbaum, J. S., Gudmundsson, H., Guo, J., Helm, V., Hofstede, C., Howat, I., Humbert, A., Jokat, W., Karlsson, N. B., Lee, W. S., Matsuoka, K., Millan, R., Mouginot, J., Paden, J., Pattyn, F., Roberts, J., Rosier, S., Ruppel, A., Seroussi, H., Smith, E. C., Steinhage, D., Sun, B., van den Broeke, M. R., van Ommen, T. D., van Wessem, M., and Young, D. A.: Deep glacial troughs and stabilizing ridges unveiled beneath the margins of the Antarctic ice sheet, Nature Geoscience, 13, 132–137, https://doi.org/10.1038/s41561-019-0510-8, 2020.

Young, T. J., Schroeder, D. M., Christoffersen, P., Lok, L. B., Nicholls, K. W., Brennan, P. V., Doyle, S. H., Hubbard, B., and Hubbard, A.: Resolving the internal and basal geometry of ice masses using imaging phase-sensitive radar, Journal of Glaciology, 64, 649–660, https://doi.org/10.1017/jog.2018.54, 2018.